IIII Original Paper IIII

A Microgravity Environment Improves Structural Resolution and Endows Cues for Specific Inhibition of Mitogen-Activated Protein Kinase Kinase 7

Takayoshi KINOSHITA[1], Takuma HASHIMOTO[1], Yuka MURAKAWA[1], Yuri SOGABE[1],
Takashi MATSUMOTO[2] and Masaaki SAWA[3]

Abstract

Mitogen-activated protein kinase kinase 7 (MAP2K7) regulates stress and inflammatory responses, and is an attractive drug discovery target for serious diseases such as arthritis and cardiac hypertrophy. A microgravity environment improved the crystal quality of MAP2K7 and improved the structural resolution to 1.3 Å. High resolution analysis structurally clarified the two regions, which were undefined in the previous low-resolution analysis and conferred structural insights for producing MAP2K7-specific inhibitors. The hinge region alternatively configures the canonical and atypical conformations. The latter could allow binding MAP2K7 inhibitors with a novel scaffold. The C-terminal region works as a negative regulator with intermolecular association, which implies the ability to produce highly selective MAP2K7 inhibitors.

Keyword(s): MAP2K7, High-resolution structure, Crystallization in microgravity, Allosteric regulation, Specific inhibition.
Received 30 October 2018, Accepted 19 December 2018, Published 31 January 2019.

1. Introduction

Mitogen-activated protein kinase kinase 7 (MAP2K7) plays a crucial role in the c-Jun N-terminal kinase (JNK) signaling cascade, which regulates stress and inflammatory responses [1], and is an attractive drug discovery target for serious diseases, including arthritis, hepatoma, and cardiac hypertrophy [2–4]. The selectivity of MAP2K7 inhibitors against other kinases, in particular MAP2Ks (MAP2K1–MAP2K6), is a primary barrier in drug development. High-resolution crystal structures of MAP2K7 could overcome this issue. In the first stage, we solved the wild-type structure of MAP2K7 at 3.0 Å resolution using the molecular replacement method [5]. This structure involved several undefined regions because of the low resolution. After that, the chemical stabilization of the MAP2K7 protein by the mutation of a surface cysteine to serine (C218S) drastically augmented the crystallographic resolution to 2.1 Å and improved the structural accuracy [6]. However, the undefined regions in this structure remained, involving the N- and C-terminals, and activation loop (A-loop), which is regulated by phosphorylation and works as a platform for the substrate binding. The poor definition of these regions was likely due to the model bias and/or multiple conformations. Finally, the C218S crystals grown under microgravity in a space environment yielded a 1.3-Å resolution structure, clarifying the ambiguous regions in the latest analyses, and identifying the multiple conformations [7]. The outline in this high-resolution structure has been reported as a short communication [7]. In this paper, we will dissect this structure using the additional biochemical data and depict the crucial cues for producing MAP2K7-specific inhibitors.

2. Experimental

2.1 Crystallization and Structure Analysis

The C218S mutant of MAP2K7 was prepared and crystallized with the ATP analogue under the same conditions as the wild type [5, 6]. Under a microgravity environment, crystals were obtained at 277 K, using the counter-diffusion method [8] in the Japanese Experimental Module "Kibo" at the International Space Station (ISS) [9]. The X-ray diffraction data was collected on a Quantum 270 (ADSC) at the Photon Factory BL17A beamline and integrated by HKL2000 [10]. The initial phase was determined by molecular replacement using the MAP2K7 structure (5B2K) [6] as a starting model. Structure refinement and model modification were iterated using Refmac5 [11] and Coot [12] in the CCP4 program suite [13]. The final coordinates of the C218S mutant had been deposited in the Protein Data Bank (PDB ID: 5Y90). The MAP2K7 structure was compared with those of other MAP2Ks, including MAP2K1 (PDB ID: 3EQC) [14], MAP2K2 (PDB ID: 1S9I) [15], MAP2K4 (PDB ID: 3ALO) [16], and MAP2K6 (PDB ID: 3VN9) [17].

2.2 Cascade Kinase Assay

Cascade kinase reactions were conducted in a solution containing active mitogen-activated protein kinase kinase kinase 3 (MAP3K3) (Carna Biosciences, Kobe, Japan) as a client

1   Graduate School of Science, Osaka Prefecture University, 1-1 Gakuen-cho, Naka-ku, Sakai, Osaka 599-8531, Japan.
2   Rigaku Cooperation, Tokyo 196-8688, Japan.
3   Carna Biosciences, Inc., Hyogo 650-0047, Japan.
(*E-mail: kinotk@b.s.osakafu-u.ac.jp)

kinase of MAP2K4, inactive MAP2K4 prepared by the reported procedure [16], unphosphorylated GST-tagged JNK1 (Carna Biosciences) as the substrate, 20 mM Tris-HCl, pH 7.5, 3 mM MgCl$_2$, and 25 μM ATP at room temperature. Phosphorylated JNK1 was detected by an anti-phospho-pJNK1 monoclonal antibody (Merck Millipore, Burlington, MA, USA) as the primary antibody on a glutathione-coated ELISA plate (Thermo Fisher Scientific, Waltham, MA, USA). The amount of immunocomplexes was detected using 3,3',5,5'-tetramethylbenzidine (TMB) chemical luminescence evoked by horseradish peroxidase conjugated to a goat anti-mouse IgG antibody (Thermo Fisher Scientific) as the secondary antibody. The inhibitory activity of the C-peptide for MAP2K4 was measured at 0.01 – 1 mM.

3. Results and Discussion

3.1 Structural Dissection of MAP2K7 at the High Resolution

The 1.3-Å resolution (high resolution) structure of MAP2K7 conserved a typical kinase fold, consisting of the N- and C-lobes and the hinge region linking these lobes (**Fig. 1**), and depicted the DFG-out conformation, i.e., an auto-inhibition state, without ATP analogue binding. Generally, a kind of the inhibitors such as imatinib induces the DFG-out conformation, in which the peptide group between the aspartate and phenylalanine residues in the DFG motif was flipped and the ability to bind the ATP and substrate was completely lost [19]. Additional 275 water and 3 glycerol molecules could be assigned in the high-resolution structure compared with the 2.1-Å resolution structure.

While the 2.1-Å resolution structure of MAP2K7 had involved three undefined regions, the high-resolution structure delineated 2 and 13 residues in the N- and C-terminal regions, respectively, but not in the activation loop. Model bias in the both terminal regions was removed by the augment of X-ray diffraction data. On the other hand, the activation loop remained poorly defined even at high resolution. The result suggests that this region is entirely disordered (**Fig. 1**).

The high-resolution structure also showed flexible residues with multiple conformations, which were analyzed as a single conformation in the lower resolution structure (**Table 1**). The alternative conformations of the side chain were observed in the 15 residues on the surface of MAP2K7. Two regions, a loop in

Table 1 Multiple conformations observed in the high-resolution structure.

Side chain	Q127, Q130, M142, K165, R178, N205, K237, D259, R270, Q272, M300, K350, E354, K389, R398
Main chain	M215-G216-T217 (in the hinge region) P357-L358 (in the bottom of the C-lobe)

the bottom of the C-lobe and hinge region, were defined by the alternative conformations in the main chains.

3.2 Cues for Producing Specific Inhibitors

More than 20 water molecules were found around the predictive ATP binding site in the high-resolution structure, although only two water molecules could be assigned in the 2.1-Å resolution structure. These water-molecule-binding sites are greatly informative for the design of MAP2K7 inhibitors. The glycerol molecules were found in the top of the N-lobe or the bottom of the C-lobe. The structural insight regarding glycerol is presumably useful for producing allosteric MAP2K7 inhibitors.

The alternative conformations in the main chains of MAP2K7 were observed in the hinge region which is significant for binding the adenine moiety of ATP or the various heterocyclic moieties of ATP-competitive inhibitors. Gly216 in the middle of the hinge region of MAP2K7 likely allows for this structural alternation, as in a p38α kinase observed previously[18]. The main chains in the hinge region take part in hydrogen-bonding with the adenine or heterocyclic moiety. Therefore, the flexibility in the hinge region of MAP2K7 likely raises the possibility to discover novel compounds with an atypical moiety as a kinase inhibitor. Furthermore, these compounds probably have potential to be highly selective to the other MAP2K because Gly216 of MAP2K7 is unique among MAP2Ks (2K4: serine, 2K1, 2K2, 2K3, 2K5, and 2K7: aspartate).

The defined C-terminal region of MAP2K7 bound to a slot in the N-lobe of the adjacent molecule (**Fig. 2**). The region of Gly424-His430 with an extended configuration interacted with the cleft in the N-lobe via the hydrogen bonds and hydrophobic interactions (**Fig. 2**). The main chains of Val425, Ser427, and His430 in the C-terminal region took part in three hydrogen
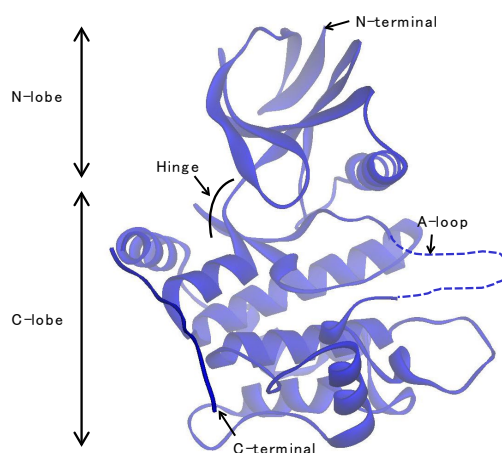
Fig. 1 Overall structure of MAP2K7 at high resolution. The disordered region is shown by a dotted line.
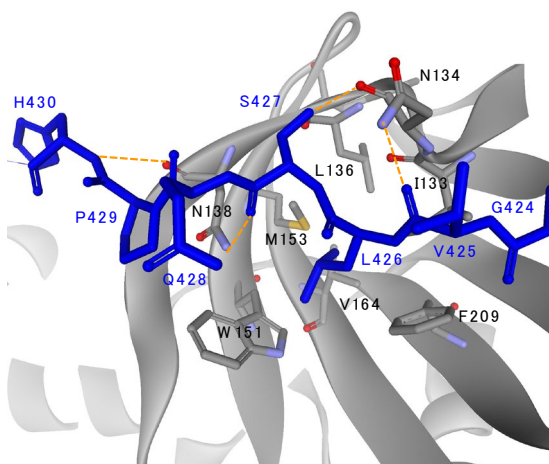
Fig. 2 Intermolecular interaction of MAP2K7. The C-terminal region of MAP2K7 (navy) binds to the N-lobe of the adjacent molecule. Hydrogen bonds are shown by orange dotted lines.

Table 2 Amino acid residues important for the Leu426 pocket of MAP2Ks.

MAP2K7	Asn138	Trp151	Val164
2K1	Lys	Phe	Arg
2K2	Arg	Thr	Arg
2K3	Thr	Glu	Val
2K4	Asp	Asn	Val
2K5	Tyr	Tyr	Val
2K6	Pro	Glu	Val

bonds, and the Oγ atom of Ser427 made a hydrogen bond with the main chain carbonyl group of Asn134 of the adjacent molecule (**Fig. 2**). Pro429 formed van der Waals interactions with the side chain of Asn138. The side chain of Leu426 in the middle of the C-terminal region intruded into the deep hydrophobic pocket formed by Ile133, Leu136, Trp151, Met153, Val164, and Phe209 (**Fig. 2**). The indole group of Trp151 made a CH-π like interaction with the Cδ atom of Leu426. This intermolecular interaction likely contributed to the induction of the DFG-out conformation. The cascade kinase assay was used to evaluate the biological effect of the C-terminal region on the enzyme activity. The synthesized Thr422-His430 peptide (C-peptide) inhibited with an IC$_{50}$ value of 100 μM [7]. These results revealed that the C-terminal region functions as an allosteric negative regulator of MAP2K7 by shifting to the DFG-out state, a well-known auto-inhibition state.

3.3 Selectivity of C-Peptide for MAP2K7

The C-terminal region of MAP2K7 is much longer than the other MAP2K and not conserved among MAP2K. Therefore, the regulatory function of the C-terminal region is likely specific for MAP2K7. Therefore, we structurally and biochemically investigated the selectivity of C-peptide against the other MAP2Ks.

The structural dissection indicates that the hydrophobic pocket accommodating Leu426, referred as to the Leu426 pocket, is essential for the C-terminal region binding to the N-lobe. In particular, Asn138, Trp151, and Val164 forming the pocket likely contribute to the specific intermolecular interaction. Trp151 and Val164 collaboratively construct the bottom of the pocket and the former closely interacts with Leu426. Asn138 forms the side wall of the pocket, but also tightly interacts with Pro429 and makes a hydrogen bond (**Fig. 2**). The other

MAP2Ks would neither form the Leu426 pocket due to the amino acid difference as shown in **Table 2**, nor bind C-peptide. In MAP2K1 and MAP2K2, arginine residue corresponding to Val164 of MAP2K7 fulfilled the Leu426 pocket, although aromatic amino acid was conserved at the Trp151 site (**Table 2**, **Figs. 3a**, **3b**). Furthermore, lysine or arginine residue at the Asn138 site could not form the hydrogen bond observed in MAP2K7. In MAP2K4 and MAP2K6, Val164 was conserved but aromatic amino acid at the Trp151 site was replaced with hydrophilic one (**Table 2**, **Figs. 3c**, **3d**). This result likely provokes a low hydrophobicity of the Leu426 pocket, and low affinity of the C-peptide to MAP2K4 and MAP2K6. MAP2K3 has glutamate residue at the Trp151 site (**Table 2**) and perhaps indicates the same propensity to MAP2K4 and MAP2K6, although the crystal structure of MAP2K3 has not been solved at present. MAP2K5 meets the requirement for the Leu426 pocket but the bulky amino acid at the Asn138 site (**Table 2**) is more likely to fulfill the pocket, although the crystal structure of MAP2K5 has not yet been solved. Altogether, the structural inspections reveal that C-peptide most likely inhibits MAP2K7 with high selectivity against the other MAP2Ks.

Crystal structures disclosed that MAP2K1, MAP2K2, and MAP2K6 did not possess the cavity tolerable for the peptide binding in the N-lobe, but MAP2K4, a client kinase to JNKs identically to MAP2K7, bound the substrate peptide or N-terminal region of the adjacent molecule at the common site of the N-lobe [16]. This N-lobe binding site in MAP2K4 lies far apart from that of MAP2K7 (**Figs. 2**, **3c**). These suggest that MAP2K4 likely equips the N-lobe regulatory system distinct from MAP2K7. However, the C-peptide displayed no inhibitory activity to MAP2K4 at the high concentration of 1 mM.

4. Conclusion

Crystals of the C218S mutant grown under a microgravity environment conferred a 1.3- Å structure of MAP2K7. This high-resolution structure encompassed the worthwhile cues for producing novel and specific MAP2K7 inhibitors. The atypical conformation in the hinge region due to Gly216 would enable novel moieties to bind at the ATP binding site of MAP2K7. These compounds likely display high selectivity for MAP2K7
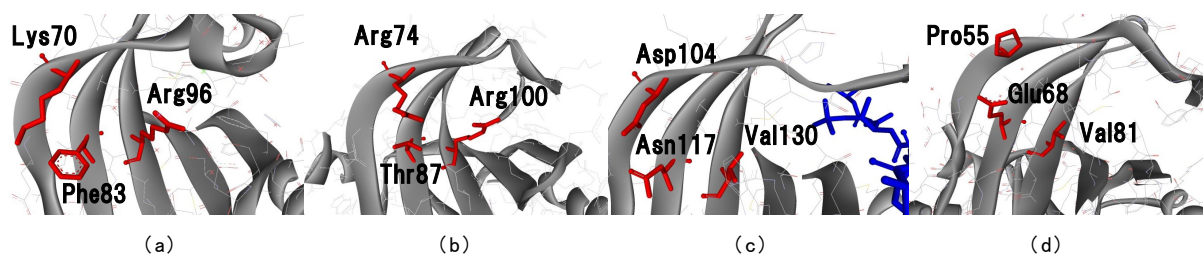
Fig. 3 The Leu426 pocket region of the N-lobe in MAP2Ks. The residues located at the sites essential for the formation of the Leu426 pocket are shown in red. a) MAP2K1. b) MAP2K2. c) MAP2K4. The substrate peptide (navy) binds to the site far from the Leu426 pocket. d) MAP2K6.

because Gly216 is unique among MAP2Ks. Furthermore, the C-terminal region unique to MAP2K7 bound to the N-lobe of the adjacent molecule and is seemed to down-regulate the enzyme activity with an allosteric manner. The synthesized C-terminal peptide moderately inhibited MAP2K7 with the high selectivity against MAP2K4, a closest homologue of MAP2K7. Together all, the structural and biochemical insights indicated that the C-terminal peptide was qualified as a seed compound with the high selectivity for the anti-MAP2K7 drug discovery.

Acknowledgments

References

1) M.A. Bodoyevitch: BioEssays, **28** (2006) 923.
2) S. Lee, D.L. Boyle, A. Berdeja and G.F. Firestein: Arthritis Res. Ther., **14-R38** (2012) 1.
3) B. Tang, J. Du, J. Wang, G. Tan, Z. Wang and L. Wang: Oncol. Rep., **27** (2012) 1090.
4) J. Wang, H. Wang, J. Chen, X. Wang, K. Sun, Y. Wang, J. Wang, X. Yang, X. Song, Y. Xin, Z. Liu and R. Hui: Biochem. Biophys. Res. Commun., **372** (2008) 623.
5) Y. Sogabe, T. Matsumoto, T. Hashimoto, Y. Kirii, M. Sawa and T. Kinoshita: Bioorg. Med. Chem. Lett., **25** (2015) 593.
6) Y. Sogabe, T. Hashimoto, T. Matsumoto, Y. Kirii, M. Sawa and T. Kinoshita: Biochem. Biophys. Res. Commun., **473** (2016) 476.
7) T. Kinoshita, T. Hashimoto, Y. Sogabe, H. Fukada, T. Matsumoto and M. Sawa: Biochem. Biophys. Res. Commun., **493** (2017) 313.
8) J.M. Gracia-Ruiz and A. Morena: Acta Crys., **D50** (1994) 484.
9) S. Takahashi, K. Ohta, N. Funabashi, B. Yan, M. Koga, Y. Wada, M. Yamada, H. Tanaka, H. Miyoshi, T. Kobayashi and S. Kamibachi: J. Synchrotron Radiat., **20** (2013) 968.
10) Z. Otwinowski and W. Minor: Method in Enzymology, ed. C.W. Carter, Jr. & R.M. Sweet, 276/part A, 307, Academic Press, New York, 1997.
11) G.N. Murshudov, R. Skubak, A.A. Lebedev, N.S. Pannu, R.A. Nicholis, M.D. Winn, F. Long and A.A. Vagin: Acta Cryst., **D67** (2011) 355.
12) P. Emsley and K. Cowtan: Acta Cryst., **D60** (2004) 2126.
13) M.D. Winn, C.C. Ballard, K.D. Cowtan, E.J. Dodson, P. Emsley, P.R. Evans, R.M. Keegan, E.B. Krissinel, A.G. Leslie, A. McCoy, S.J. McMicholas, G.N. Murshudov, N.S. Pannu, E.A. Potterton, H.R. Powell, R.J. Read, A. Vagin and K.S. Wilson: Acta Cryst., **D67** (2011) 235.
14) T.O. Fischmann, C.K. Smith, T.W. Mayhood, J.E. Myers, P. Reichert, A. Mannarino, D. Carr, H. Zhu, J. Wong, R.S. Yang, H.V. Le and V.S. Madison: Biochemistry, **48** (2009) 2661.
15) J.F. Ohren, H. Chen, A. Pavlovsky, C. Whitehead, E. Zhang, P. Kuffa, C. Yan, P. McConnell, C. Spessard, C. Banotai, W.T. Mueller, A. Delaney, C. Omer, J. Sebolt-Leopold, D.T. Dudley, I.K. Leung, C. Flamme, J. Kaufman, S. Barrett, H. Tecle and C.A. Hasemann: Nat. Struct. Mol. Biol., **11** (2004) 1192.
16) T. Matsumoto, T. Kinoshita, Y. Kirii, K. Yokota, K. Hamada and T. Tada: Biochem. Biophys. Res. Commun., **400** (2010) 369.
17) T. Matsumoto, T. Kinoshita, H. Matsuzaka, R. Nakai, Y. Kirii, K. Yokota and T. Tada: J. Biochem., **151** (2012) 541.
18) C.E. Fitzgerald, S.B. Patel, J.W. Becker, P.M. Cameron, D. Zaller, V.B. Pikounis, S.J. O'Keefe and G. Scapin: Nat. Struct. Mol. Biol., **10** (2003) 764.
19) T. Schindler, W. Bornmann, P. Pellicena, W.T. Miller, B. Clakson and J. Kuriyan: Science, **289** (2000) 1938.